

# INVESTIGATION OF HELIUM ACCUMULATION IN IMPLANTED ODS STEELS

*J. Simeg Veternikova<sup>1</sup>, V. Slugen<sup>1</sup>, M. Fides<sup>2</sup>, J. Degmova<sup>1</sup>, M. Petriska<sup>1</sup>, S. Sojak<sup>1</sup>*

<sup>1</sup> *Institute of Nuclear and Physical Engineering, Faculty of Electrical and Information Technology, Slovak University of Technology, Ilkovicova 3, 812 19 Bratislava*

<sup>2</sup> *Institute of Materials Research, Slovak Academy of Sciences, Watsonova 47, 04001 Kosice*

*E-mail: jana.veternikova@stuba.sk*

*Received 30 April 2017; accepted 07 May 2017*

## 1. Introduction

The newest generation of nuclear reactors (GEN IV) with planned outlet temperature up to or even over 500 °C needs more radiation and thermal resistant materials than recently used reactors. Some of them also require high corrosion resistance in different cooling media as supercritical water, molten salt, etc. Research and development of construction materials have run along with the development of the reactors, however the final decision about the material for some components is still missing.

In this paper, the new perspective materials - oxide dispersion strengthened (ODS) steels with high chromium content are investigated as possible candidates for construction of fuel cladding and internal components, mostly in reactors with more aggressive chemical environment. These steels are typical by high strength and thermal resistance. They have also better corrosion resistance due to higher chromium content (between 14 - 20 wt.% Cr).

The high chromium ODS steels have already been tested couple times to radiation resistance by many ways [1-4]. The investigation of complex materials is quite difficult and sensitive task due to their complicate and inhomogeneous structure, thus the examination of model alloys is mostly preferred round the world or simulation works of ODS structure are common [5-9]. Therefore, more details are still missing within the radiation study of ODS steels; formation of helium bubbles and their influence included.

Our work was focused on the irradiation of the commercial ODS steels (MA 956, ODM 751 and MA 957) by helium ions and study of their microstructural changes in term of vacancy defects, helium presence and hardness up to the depth of 1.2 μm. The main purpose of our work was to detect helium in structure of implanted high chromium ODS steels.

## 2. Investigated samples and experimental techniques

The investigated samples were prepared from the three different high chromium ODS steels – MA 956, MA 957 and ODM 751 obtained as commercial products of different international metal corporations. The steel MA 956 is a commercial product of company Incoloy, firstly developed for space and air industry. MA 957 is a commercial ferritic ODS alloy with 14 wt. % Cr originally developed by company INCO at 1970's. The ODM 751 is Fe-Cr-Al alloy prepared by company Dour Metal as steel with special no-typical “onion skin” ODS structure. The chemical composition of the investigated steels was tested by optical emission spectroscopy at the Welding Research Institute in Bratislava and is listed in Table 1.

Tab. 1 *Chemical composition of investigated ODS steels in wt. %.*

Alloys	C	Mn	Si	Ni	Cr	Mo	Ti	Al	O	Y
MA 956	0.03	0.06	0.05	0.11	21.7	0.05	0.33	5.77	0.21	0.38
ODM 751	0.07	0.07	0.06	0.02	16.1	1.7	0.7	3.8	0.21	0.38
MA 957	0.03	0.09	0.04	0.13	13.7	0.03	0.98	0.03	0.21	0.28

The steels were prepared by the standard processes of sintering and mechanical alloying defined by the producers. The samples were prepared from as-received material by cutting the steel sheets into suitable pieces with diameter  $10 \times 10 \times 0.8 \text{ mm}^3$ . In order to remove surface impurities, the sample surfaces were polished after the cutting almost into a mirror level. The zone affected by cutting usually goes around  $150 \mu\text{m}$  [10], but subsequent grinding removes the most affected subsurface and the powder used for polishing of our samples had particles with size of  $0.5 \mu\text{m}$ . The roughness of the as-received samples surface measured by atomic force microscopy achieved up to  $50 \text{ nm}$ , thus the influence of the sample preparation is probably for the subsurface techniques minimal.

The samples were loaded by radiation damage performed at a linear accelerator belonging to the Institute of Nuclear and Physical Engineering, Slovak University of Technology. Helium ions ( $\text{He}^{2+}$ ) with a kinetic energy up to  $500 \text{ keV}$  were implanted into the samples. During the ion implantation, point defects accumulate into the structure as a result of the atom knocking-on by the helium nuclei [11]. Therefore accumulation of small vacancy defects typical for ferritic structure was assumed in the investigated steel which should be leading to a small increase of its hardness for sufficient damage. The implanted helium is also accumulated in the structure and can be placed in defects.

The implantation temperature achieved maximum of  $62 \text{ }^\circ\text{C}$ ; therefore it has no effect on the structure. The implantation level was  $\sim 1 \times 10^{18} \text{ ions cm}^{-2}$  and the maximum radiation damage was calculated by SRIM [12] around  $45 \text{ dpa}$  for the damaged zone. The maximum of the radiation induced defects are assumed in depth of  $\sim 900 \text{ nm}$  (Fig. 1). The highest helium concentration should be in depth of around  $1 \mu\text{m}$ . These two peaks situated in different depths could be used for observation of defects and helium accumulation separately by application of slow positron beam and nanoindentation with variable investigation depths.

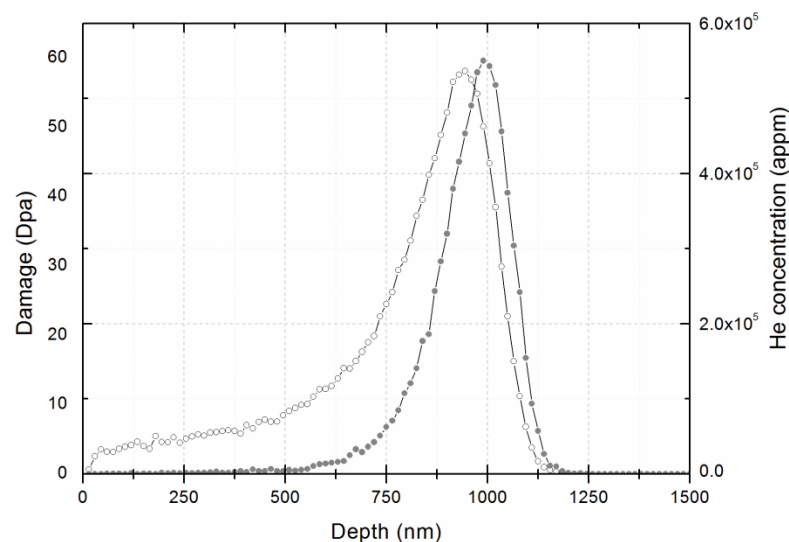


Fig. 1 SRIM calculation of radiation damage (DPA) and helium accumulation (He) for Fe-15Cr model.

The samples were investigated by positron Doppler broadening spectroscopy applied with slow positron beam sensitive to surface and subsurface layers. The momentum distribution of Doppler broadening spectra [13] was observed after helium ion implantation and its behaviour was further discussed. The standard treated data have been published in [14] and have showed increased S parameter for all implanted samples explained as visible defect accumulation. In this paper, the DBS data are analyzed according to the method published in [15], where we proved that the presence of helium can be observed in helium implanted samples by an application of positron spectroscopy.

The DBS technique [16] with a conventional setup was applied during the measurement and DBS spectra were recorded by one HPGe detector with Gaussian resolution function of 1.24 keV. The monoenergetic beam can achieve energies ranging from 0.5 to 36 keV which allows measurements from surface to 1.6  $\mu\text{m}$  [13].

The depth profile of nanoindentation was measured for purpose of completing the positron data, as mechanical properties (hardness included) should reflect the structural changes in materials. The measurement of nanoindentation was performed at Slovak Academy of Sciences by Agilent Nano Indenter G200 hardness tester at room temperature. The tests were evaluated by the standard method of Oliver and Pharr [17]. The Berkovich indenter was used for hardness measurement (HIT) up to the depth of 2000 nm with velocity of 30 nm/s. The applied load was approx. up to 600 mN and 16 depth profiles were measured from which average values of hardness were calculated.

### 3. Results and discussion

The positron data shown in Fig. 2 are displaying the rate of momentum distribution of positron annihilation spectra for implanted and non-implanted samples in two different depths - 940 nm and 1000 nm. According to the theory, the depth of 940 nm should be typical for the maximum of the radiation damage expressed as the maximum concentration of vacancy defects. The depth of 1000 nm contains probably the highest concentration of helium accumulated due to the implantation. The measured data of MA 956 are in agreement with the assumption; the ratio up to  $5 \times 10^{-3} m_0c$  (S parameter) in 940 nm is higher than in 1000 nm, which characterized bigger radiation damage. On the other hand, the ratio in depth 1000 nm is higher in area between (10 and 15)  $\times 10^{-3} m_0c$ . This suggested significant helium presence as was published in [15].

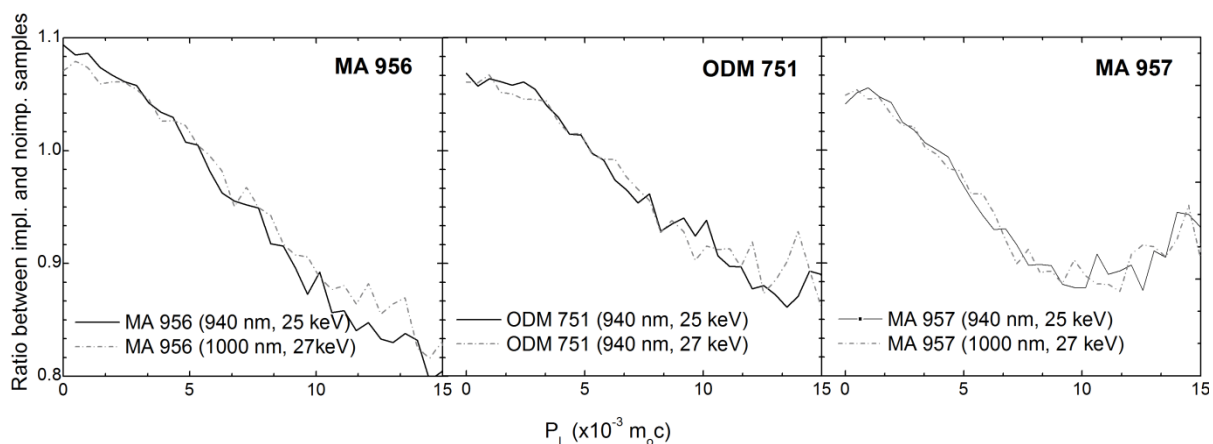


Fig. 2 Results from positron Doppler broadening spectroscopy treated for electron momentum ( $p_L$ ).

However, the other ODS steels ODM 751 and MA 957 have not values confirming the helium accumulation in the depth 1000 nm and the S parameter also shows similar damage in both layers. This can be explained by better resistance of MA957 and ODM751 to helium accumulation or helium accumulated more probably in different layers. Thus the S parameter was not suppressed by helium presence in data for the layer in 1000 nm. The nanoindentation can give better understanding.

After the implantation, the hardness increase ( $\Delta H_{IT}$ ) was quite well visible in the steels MA 957 and ODM 751 (up to 20 %), but almost no changes were observed in MA 956 (Fig. 3). The values of hardness for the MA 957 have bigger dispersion (mostly in the non-

implanted state) which can demonstrate bigger structural inhomogeneity than for the other investigated steels. The change of hardness due to the implantation was visible only between 0.1 and 1.1  $\mu\text{m}$ , which is in a good agreement with the theory.

The steels MA 957 and ODM 751 have the biggest increase of hardness in layers up to 500 nm, which can be an effect of the defects as well as helium accumulation. The defects with helium located in them are more stable and are not able to diffuse or relax. This can support positron data and explanation that helium was able to accumulate or be trapped within the layers closer to surface in compare to the expected depth. Further, the visible change of hardness could be also due to secondary knocked-on atoms which higher energy closer to the surface.

The hardness of MA 956 is similar almost for the whole range, except of deeper layers from 750 nm where implanted sample is slightly harder. This could be due to higher helium concentration there. However, the steel MA 956 have been at the same time affected by blistering effect [18] removing the first surface layers in some part of the sample which affected and distorted the results.

The increase of the average hardness calculated from 16 measurements was:  $0.7 \pm 0.5$  for ODM 751,  $2.5 \pm 1.9$  for MA 957 and about  $0.2 \pm 1.6$  for MA 956.

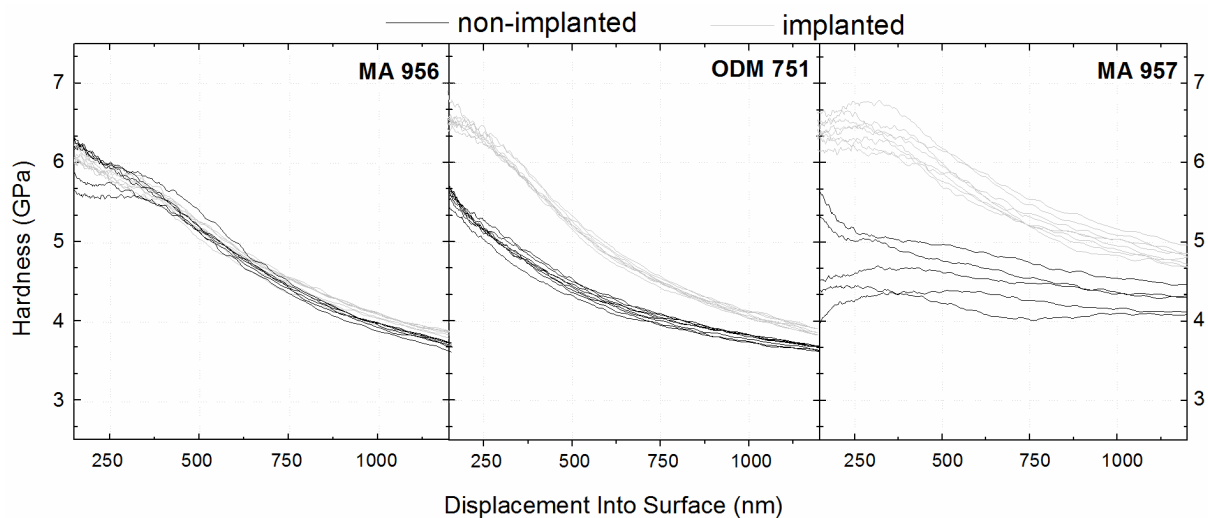


Fig. 3 *Hardness depth profile.*

#### 4. Conclusion

This paper studied the helium accumulation in microstructure of helium implanted ODS steels. During the research we applied new published methods of positron annihilation spectra treatment, but the data showed different results than was assumed. The steel MA 956 was in a good agreement with the data for Fe-9Cr model alloys, thus helium was probably accumulated in the depth of 1000 nm, which was confirmed also by a strong blistering effect in this layers and approx. 1  $\mu\text{m}$  thick layer was removed just due to helium accumulation in vacancy defects and helium bubbles formation. On the other hand, the steels MA 957 and ODM 751 did not demonstrated visibly helium in positron data. However, from the hardness measurement we assume that helium could have been accumulated and trapped in layers closer to subsurface, which is not able to detect further by positron measurements due to overlapping of the radiation and helium peaks.

## Acknowledgement

This work was supported by Slovak National Grant VEGA 1/0104/17, VEGA 1/0339/16 and VEGA 1/0477/16. This work was also realized within the frame of the project „Infrastructure Improving of Centre of Excellence of Advanced Materials with Nano- and Submicron-Structure“, ITMS 26220120035, supported by the Operational Program “Research and Development” financed through European Regional Development Fund.

## References:

- [1] M. A. Pouchon, J. Chen, M. Dobeli, W. Hoeffelner: *J. Nucl. Matter.* **352** (2006) 57–61.
- [2] K. Yutani, H. Kishimoto, R. Kasada, A. Kimura: *J. Nucl. Matter.* **367 – 370** (2007) 423–427.
- [3] M. B. Toloczko, F.A. Garner, S.A. Maloy: *J. Nucl. Matter.* **428** (2012) 170–175.
- [4] J. Ribis: *J. Nucl. Matter.* **434** (2013) 178–188.
- [5] C.L. Chen, A. Richter, R. Kogler: *Journal of Alloys and Compounds* **586** (2014) S173–S179
- [6] C. Robertson, B.K. Panigrahi, S. Balaji, S. Kataria, Y. Serruys, M.H. Mathon, C.S. Sundar: *J. Nucl. Matter.* **426** (2012) 240–246.
- [7] D.A. McClintock, M. A. Sokolov, D.T. Hoelzer, R.K. Nanstad: *J. Nucl. Matter.* **392** (2009) 353–359.
- [8] H. Kishimoto, K. Yutani, R. Kasada, O. Hashitomi, A. Kimura: *J. Nucl. Matter.* **367–370** (2007) 179–184.
- [9] N. Baluc, J. L. Boutard, S. L. Dudarev, M. Rieth, J. Brito Correia, B. Fournier, J. Henry, F. Legendre, T. Leguey, M. Lewandowska, R. Lindau, E. Marquis, A. Muñoz, B. Radiguet, Z. Oksiuta: *J. Nucl. Matter.* **417** (2011) 149–153.
- [10] P. Horodek, J. Dryzek, M. Wrobel, *Tribol Lett* **45** (2012) 341.
- [11] G. Kinchin, R. Pease: *Rep. Progr. Phys.* **18** (1955) 1-51.
- [12] J.F. Ziegler, The stopping and range of ions in solids, Pergamon, New York, 1985, pp. 321. ISBN 13: 978-0080216034.
- [13] R. Krause-Rehberg, S. H. Leipner, Positron annihilation in Semiconductors, second ed., Springer, Berlin, 1998. ISBN 3-540-64371-0.
- [14] J. Simeg Veternikova, V. Slugen, S. Sojak, M. Skarba, E. Korhonen, S. Stancek, J. Degmova, V. Sabelova, I. Batosova, *J. Nucl. Mat.* **450** (2014) 99-103.
- [15] V. Sabelova, V. Krsjak, J. Kuriplach, M. Petriska, V. Slugen, J. Simeg Veternikova, *J. Nucl. Mat.* **450** (2014) 54-58.
- [16] M. J. Puska, R. M. Nieminen, Theory of positrons in solids and on solid surfaces, *Rev. Mod. Phys.* **66** (1994) 841-893.
- [17] W.C. Oliver, G.M. Pharr: *J. Mater. Res.* **7** (1992) 1564-83.
- [18] J. Simeg Veternikova, Study of materials for advanced reactor systems, LAP Lambert, Saarbrucken, Germany, 2015, pp.129. ISBN 978-659-75823-2.